

## European Site Testing at Chajnantor: a Step Towards the Large Southern Array

A. OTÁROLA<sup>1</sup>, G. DELGADO<sup>2</sup>, R. BOOTH<sup>3</sup>, V. BELITSKY<sup>3</sup>, D. URBAIN<sup>3</sup>,  
S. RADFORD<sup>4</sup>, D. HOFSTADT<sup>1</sup>, L. NYMAN<sup>2</sup>, P. SHAVER<sup>1</sup>, R. HILLS<sup>5</sup>

<sup>1</sup>European Southern Observatory; <sup>2</sup>SEST/Onsala Space Observatory; <sup>3</sup>Onsala Space Observatory;  
<sup>4</sup>National Radio Astronomy Observatory; <sup>5</sup>Mullard Radio Astronomy Observatory

### Abstract

The Large Southern Array is one of the highest priority projects in European astronomy today. The planned submillimetre operating wavelengths and the need to maximise the efficiency of observing time make the selection of the observatory site a fundamental issue.

### 1. Introduction

The last decades have seen great progress in (sub-)millimetre astronomy, leading to the design and construction of new and powerful instruments. There are now many very good 10–15-m-diameter (sub-)millimetre telescopes available to the astronomical community. In particular, the 15-m-diameter *Swedish-ESO Submillimetre Telescope* (SEST) is unique in the Southern Hemisphere. This telescope has opened the southern skies to millimetre astronomy, achieving outstanding scientific results during the last ten years (see articles in *The Messenger* No. 91, 1998).

The continuing quest for higher resolution and greater sensitivity calls for ra-

dio telescope arrays. In 1995, European interest in a millimetre array sparked the *Large Southern Array* project (LSA) with an agreement between ESO, the *Institut de Radio Astronomie Millimétrique* (IRAM), the *Onsala Space Observatory* (OSO), and the *Netherlands Foundation for Research in Astronomy* (NFRA). With the aim of achieving a total collecting area of 10,000 m<sup>2</sup> and an angular resolution better than 0.1 arcsec at a wavelength of 3 mm, this project was at the time the most ambitious plan considered for millimetre astronomy. Since the early 1980s, the US *National Radio Astronomy Observatory* (NRAO) has planned another array, the *Millimeter Array* (MMA) which is a 2000-m<sup>2</sup> array capable of working at sub-millimetre wavelengths. Both projected instruments would be sited in northern Chile, naturally suggesting collaboration.

In 1997, ESO and NRAO agreed to work together to explore a common millimetre/submillimetre array, to be financed jointly by Europe and the US. The LSA/MMA project is a compromise array with 64 telescopes, each of 12 m diameter, giving a total collecting area of

7,000 m<sup>2</sup>, with baselines up to 10 km, and with sub-millimetre capabilities. It will be located on Llano de Chajnantor, a 5000-m-high plateau near the village of San Pedro de Atacama in the Atacama Desert area. This will be the most powerful (sub-)millimetre telescope in the world, opening completely new horizons in astronomy.

The LSA/MMA will be the natural complement, in its wavelength range, to the HST and VLT, with equivalent resolution and sensitivity and the additional capability to observe the inner part of the dust-obscured regions of star formation and dust enshrouded galaxies.

At (sub-)millimetre wavelengths, the atmosphere presents natural limits to the sensitivity and resolution of astronomical observations. Pressure-broadened molecular lines, in particular of water vapour, are the cause. The atmosphere adversely affects observations both by attenuating the incoming signal and by increasing the system noise, since it radiates thermally. Furthermore, inhomogeneities in the water vapour distribution change the electrical path length through the atmosphere. These random variations result in



Figure 1: Partial view of the site-testing equipment deployed in Llano de Chajnantor. The LSA container is to the left, while the MMA container is to the right. In the background Cerro Chascón.

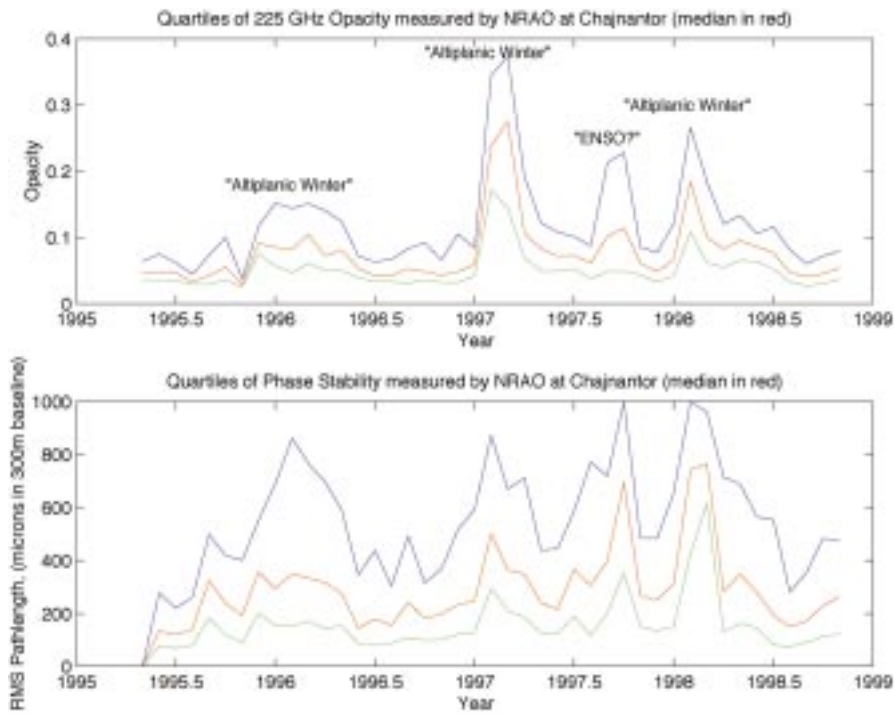


Figure 2: Quartiles of the zenith optical depth – opacity – at 225 GHz (upper plot) and the phase stability (lower plot) observed by NRAO during the years 1995–1998. The global weather conditions Altiplanic Winter and one El Niño – Southern Oscillation (ENSO) event can be seen in the cumulated data.

data, as can be seen in Figure 2. However, the Chajnantor site provides excellent observing conditions, perhaps amongst the very best in the world for sub-millimetre wavelengths. The high atmospheric transparency allows high-efficiency telescope operations.

Moreover, the whole area around Cerro Chascón, including Llano de Chajnantor, has recently been declared to be of “scientific interest” by a presidential decree. A land concession has been granted to the *Comisión Nacional de Investigación Científica y Tecnológica* (CONICYT), the agency in charge of evaluating, supporting and funding scientific and technological research in Chile. The area around the LSA/MMA is

phase errors between the array elements which degrade the sensitivity and resolution of the images. To minimise such atmospheric degradation, then, the ideal site should be a dry plateau at high altitude.

For several years the European collaboration has been exploring the northern area of Chile searching for potential sites (Otárola et al., 1996). The experience has helped not only our own efforts, but also other groups conducting site studies and/or astronomical projects in the same area. NRAO began site characterisation measurements at Llano de Chajnantor in 1995. In 1998, after more than a year of measurements at another candidate site (Pampa Pajonales), the European measurements started at Chajnantor as well. Several instruments are deployed alongside those of NRAO (Fig. 1). The goal is to share the infrastructure and to correlate the data obtained at the same place and time with the different instruments.

The work done at Chajnantor by NRAO shows that the median zenith optical depth at a frequency of 225 GHz is about 0.06 (see Fig. 2). This is significantly better than that measured at the CSO on Mauna Kea with an identical instrument. Also, there is less diurnal variation in transparency on Chajnantor than on Mauna Kea. These data span the period 1995 to 1998. The main meteorological events (“Altiplanic Winter” and “El Niño – ENSO”) have had an adverse effect on the



Figure 3: Map of the Atacama Desert region in Chile (scale 1:3,000,000). To the east of “Salar de Atacama” can be seen the location of Llano de Chajnantor, while to the south of Antofagasta Paranal can be seen (adapted from “Atlas de la República de Chile”, Instituto Geográfico Militar, 1983).

now protected from third parties and from possible mining claims or other such activities.

In this report an overview of the site, the instruments used to characterise it, their scientific rationale and some preliminary results are presented.

## 2. Chajnantor

Llano de Chajnantor is the selected site for the combined LSA/MMA project. The atmosphere at Chajnantor and the nearby plateau "Pampa La Bola" have been studied extensively by NRAO and the *Nobeyama Radio Observatory* (NRO), respectively. Measurements have shown that this area is among the driest in the world, with conditions that excel for astronomical research at several wavelengths.

Chajnantor is a 5000-m-high plateau about 60 km ESE of San Pedro de Atacama. This village is a place of great ethnological and archaeological importance, being the oldest continuously inhabited site in Chile. It is also one of the most important tourist attractions of the region because of the impressive mountain and desert landscapes, the pre-Columbian archaeological sites, the fine archaeological museum, and the relaxing atmosphere given by the rustic nature of its centuries old adobe houses and narrow streets.

### 2.1 Geomorphology

Three north-south mountain ranges dominate the geomorphology of the Atacama Desert area (see Fig. 3): the Coastal mountains, with peaks over 3500 m, the Domeyko mountains, located at middle longitudes, and the Andes, with peaks well above 5000 m.

The 25 km<sup>2</sup> Chajnantor plateau is located on the western edge of the Andes at 67°45' west and 23°01' south, about 380 km NE of Paranal. This plateau is open to the west and north-west, but several 5600-m peaks border the site in other directions.

### 2.2 Logistics

Prom Pedro de Atacama an international highway to Argentina, "Paso de Jama", allows an easy access to the site. By March 1999 this road will be paved through the CONICYT land concession, ensuring access by a good paved road.

A power source is essential for the development of the LSA/MMA. The nearest existing power lines are 180 km NW in Calama. Due to the growing commercial relations with Argentina, however, several projects are being carried out to bring natural gas from Argentina to produce electrical power for the Atacama region. One of these gas pipelines crosses the Chajnantor plateau. NRAO and GasAtacama, the pipeline owner, have signed an agreement to install a gas tap at the north edge of the Chajnantor area. This will allow the



Figure 4: One of the 183-GHz water vapour monitors to the right of the antennas of the 11.2-GHz interferometers.

LSA/MMA to generate electrical power as needed.

A few years ago, when we first started exploring this area, Chajnantor was a very isolated place. By early 1999, the site will have a good paved road running nearby and natural gas on site.

### 2.3 Climate

Weather conditions in the Atacama Desert are dominated by a high-pressure anticyclone, an inversion layer on the coast, the north-south coastal mountains, the Andes mountains, the high

insolation, and the high ventilation.

The whole area is extremely dry and lies in the meridional transition region. To the north, the Altiplano convective summer rains predominate, where frontal winter rains prevail to the south. The aridity originates in the prevailing anticyclone conditions associated with a slow downward air motion (Fuenzalida et al. 1996). Over the coast this subsidence is responsible for an inversion layer several hundred metres thick that starts about 1000 m. The inversion layer separates the moist air of the lower marine boundary layer from the dry subsiding air and acts as

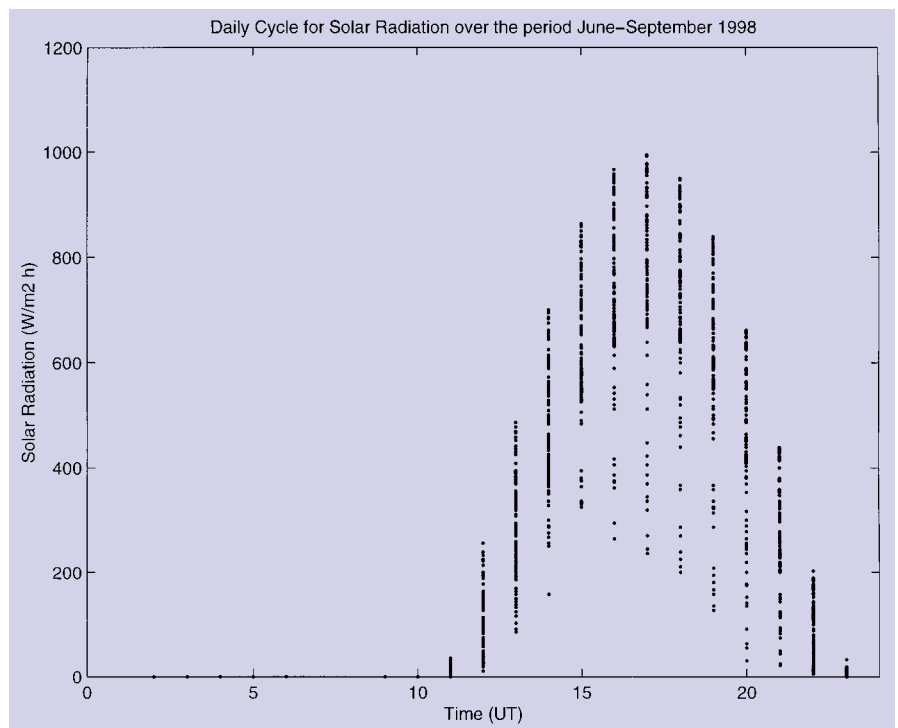


Figure 5: Diurnal cycle of the solar radiation for the period June–September 1998 in the Chajnantor area.

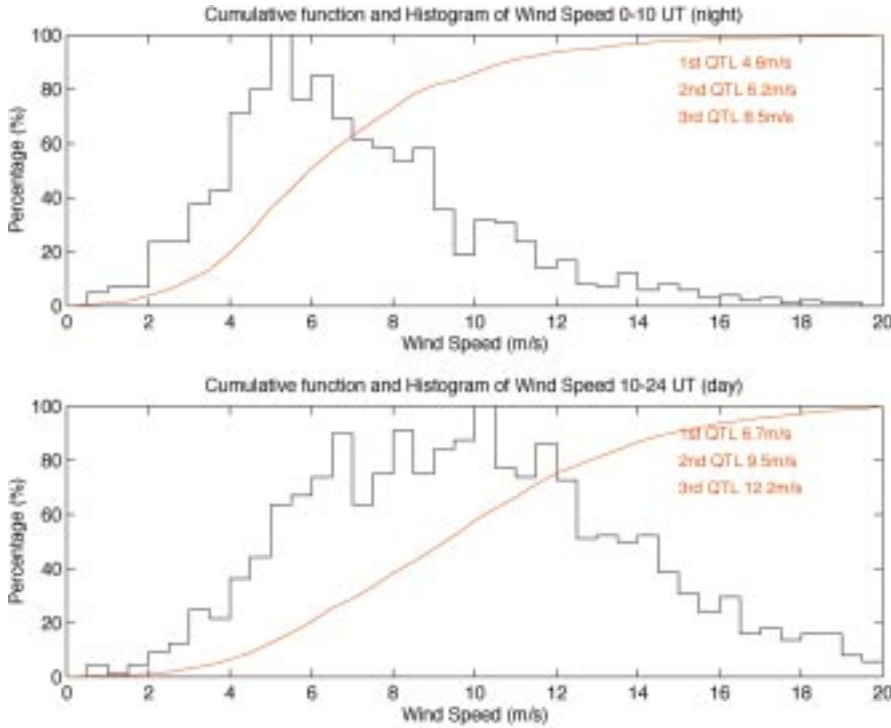


Figure 6: Cumulative function and histogram for the wind speed over the period June–September 1998 in the Chajnantor area. Upper plot shows night-time while lower one is day-time.

a barrier to any mixing process that might transport moisture evaporating from the sea to upper levels. The well-mixed marine boundary layer is restricted to lowlands along the coast on the west slope of the coastal mountain range.

As humid air masses moving westward from the Atlantic zone rise up the east slope of the Andes they cool and precipitate. Hence, very little humid air gets over to the west side of the Andes. The exception is during summer, when the high-pressure system over the Pacific weakens and, at the same time, moves southward (Fuenzalida et al. 1987, Aceituno et al. 1996). This change in atmospheric circulation allows warm humid air from the Amazon to reach the Altiplano in northern Chile and produce rain. This is known locally as “Bolivian or Altiplanic Winter”.

The driving force behind the climatological processes is the extremely high solar radiation. The daily and yearly maxima, averages and ranges of the insolation are amongst the highest recorded in the world. The average daily maximum reaches almost  $1300 \text{ W/m}^2$  during summer. Only convective and advective

processes can remove the absorbed heat because the extreme aridity means that the evaporating water cannot dissipate the heat. The wind then is the main energy carrier. The strong thermal contrast between the Pacific and the Andes drives a constant sea-mountain airflow. Almost every climatic process within the boundary layer is controlled by this regional wind system. At night the boundary layer regularly disappears so the climate near the ground is directly influenced by the upper atmosphere winds (Schmidt 1997).

### 3. Site Testing Equipment

At the beginning of June 1998, the Onsala-ESO European site-testing group deployed equipment to characterise the atmospheric conditions at Chajnantor for (sub-)millimetre astronomy. Our instrumentation and measurements complement the measurements carried out by the other groups (see Fig. 4).

#### 3.1 Container

The computers and other ancillary equipment are installed in a 20-foot in-

ulated ocean-shipping container. About  $18 \text{ m}^2$  of photovoltaic panels are mounted outside to charge a battery bank that provides about 700 W around-the-clock. The computers housed in the container control the instruments and store the data. Communications are maintained with an analogue cellular telephone. Data for all the instruments are retrieved about once a month during routine visits.

### 3.2 Weather stations

Two weather stations have been installed on the plateau. They measure air temperature, solar radiation, atmospheric pressure, relative humidity, and wind speed and direction. Their main characteristics are detailed in Table 1.

The weather stations include a data logger that, with the actual sampling rate, can store 42 days of data. The wind sensors are atop a 4-m mast and the other instruments are installed in a ventilated shelter to protect them from direct solar radiation.

Analysis of these data improves our understanding of the climatology of the site, with emphasis on the wind speed and direction and the diurnal and seasonal patterns. These data also provide information on the environmental constraints which will influence the design of the LSA/MMA antennas, and it is a basic calibration input for the analysis of the data obtained with other instruments at the site.

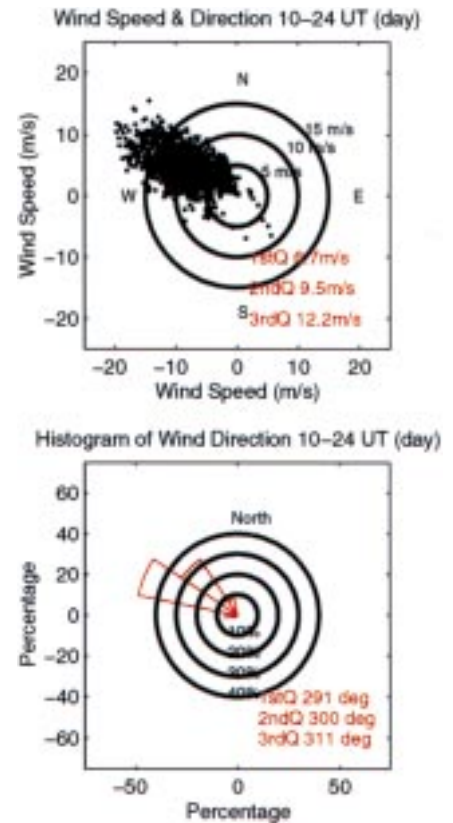


Figure 7: Wind speed and direction over 14 hours during the day (upper plot), and histogram with the percentage of time that the wind blows in a particular direction during this same time period (lower plot). The distribution for night-time is similar.

Table 1: Main characteristics of the sensors available in the weather stations deployed in Chajnantor

Sensor	Operating range	Accuracy
Air temperature	-30 – +70 °C	0.2 °C
Relative humidity	5–95%	1.5% in the range 5% to 60%
Solar radiation	0–1100 W/m <sup>2</sup>	±5% per MJoule, spectral response 400–1100 nm
Anemometer	0–150 km/h	0.5 m/s
Wind direction	0–360 degrees	3.0 degrees
Barometric pressure	740–490 mbar	±5 mbar

### 3.3 Interferometer

Atmospheric phase stability, or “seeing”, is a crucial issue for the LSA/MMA. Because radio waves travel more slowly in wet air than in dry air, fluctuations in the water vapour distribution will cause variations in the electrical path length through the atmosphere. Path length variations across the array aperture will degrade both image quality and array sensitivity. These path length fluctuations, which are almost independent of observing frequency at millimetre wavelengths, correspond to phase fluctuations that scale linearly with frequency. Simulations suggest that phase fluctuations less than 10 degrees rms at the observing wavelength will have little impact upon most images, phase errors of 30 degrees rms will permit imaging with up to 200:1 dynamic range, albeit with somewhat reduced sensitivity, and image reconstruction becomes all but impossible when phase errors exceed 60 degrees rms (Holdaway and Owen 1995b). Although the LSA/MMA will undoubtedly use a correction technique to overcome atmospheric image degradation (either fast switching or radiometric phase calibration), the better the natural stability, the better these correction schemes will work (Holdaway et al. 1995c, Woody et al. 1995).

Atmospheric phase stability at Chajnantor is monitored with two 300-m baseline interferometers observing 11.2 GHz tracking beacons broadcast by geostationary communications satellites (Radford et al. 1996). One instrument was installed by the MMA project in May 1995 and another was installed by the LSA project at Pajonales in April 1997 and later moved to Chajnantor in June 1998. Because the atmosphere is non-dispersive away from line centres, these measurements can be extrapolated to characterise the atmospheric phase stability up to at least 350 GHz and, with care, throughout the submillimetre region. These interferometers sense atmospheric structures on 300-m and smaller scales. The phase stability is characterised by the rms phase fluctuations calculated over 10-minute intervals. This interval is twenty times longer than the time it takes an atmospheric feature to move the length of the baseline at  $10 \text{ ms}^{-1}$ , which is the median wind speed aloft. Thermal instrumental phase noise is on the order of 0.1 degree rms at 11.2 GHz, while the smallest observed atmospheric phase fluctuations are – after correcting for instrumental noise – 0.3 degree rms (Holdaway et al. 1995c).

The two interferometers are collocated along the same east-west 300-m baseline, but observe different satellites separated by about  $5^\circ$ . As the (quasi-static) pattern of atmospheric turbulence passes over the interferometers, they will record similar signals that are delayed from one to the other. From this delay, some estimate of the wind speed aloft, and the geometry, we can deter-

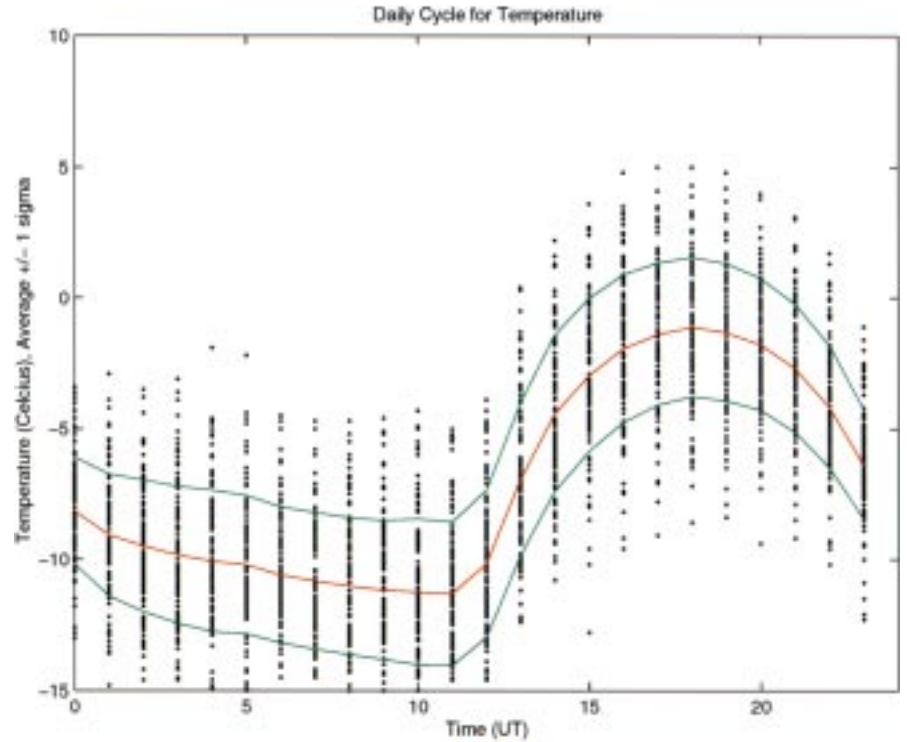


Figure 8: Diurnal temperature cycle over the period June–September 1998 in the Chajnantor area.

mine the effective height of the turbulent layer. Differences in the interferometer signals, on time scale shorter than the delay, provides a measure of the evolution of the turbulence (Holdaway and Radford 1998). The effectiveness of fast switching at overcoming atmospheric image degradation depends on both the height and the time scale for evolution of the turbulence (Holdaway and Owen 1995b).

### 3.4 183 GHz water vapour monitor

Now under development at several observatories, water-line radiometry is a promising technique for overcoming the effects of atmospheric phase fluctuations. The varying depth of the water vapour column is determined by continuously monitoring the intensity and shape of a water-vapour emission line. Changes in the atmospheric phase delay are then

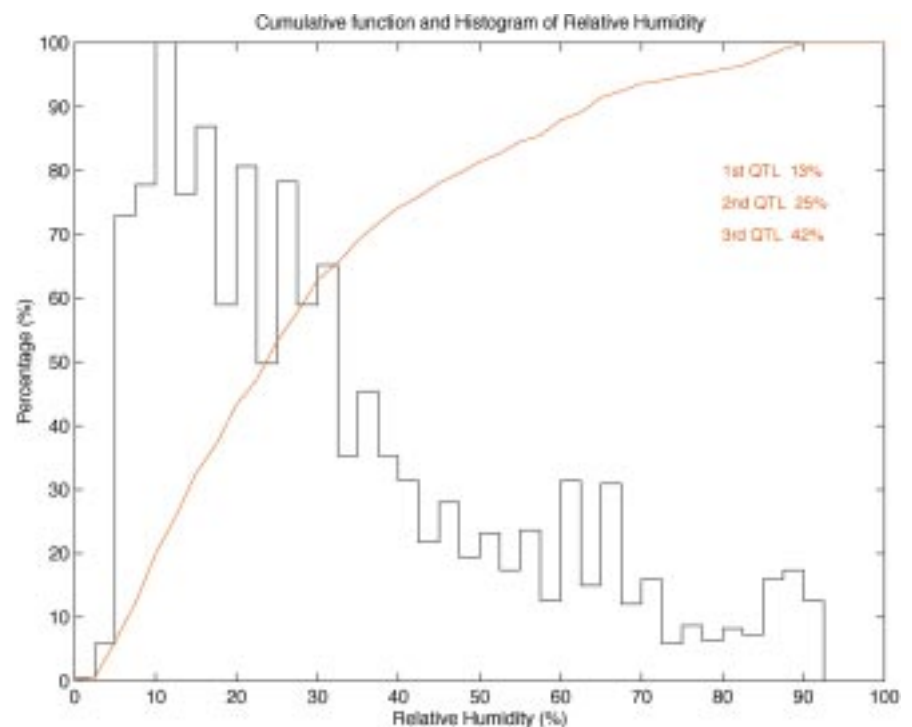


Figure 9: Cumulative function and histogram for the relative humidity over the period June–September 1998 in the Chajnantor area.

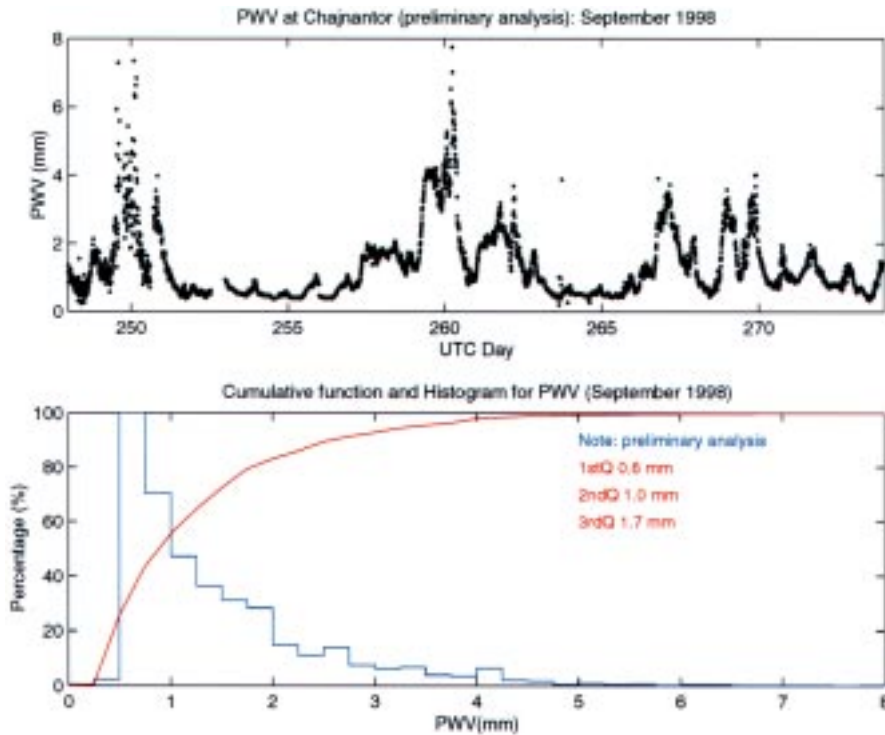


Figure 10: Amount of precipitable water vapour content during the month of September 1998 in the Chajnantor area (upper plot), and cumulative function and histogram for the same month (lower plot). Several storms affecting the area can be seen.

determined and used to improve the astronomical images. Both the 22 GHz and the 183 GHz line are candidates for this method, but it is not yet clear which is best for the conditions at Chajnantor.

Two radiometers for the 183 GHz water-vapour line have been built as a collaborative project between *Onsala Space Observatory*, through the *Group for Advanced Receiver Development* at *Chalmers University of Technology*, and the *Mullard Radio Astronomy Observatory (MRAO)*, *Cavendish Laboratory*, Cambridge. They have been installed at Llano de Chajnantor at the ends of the 300-m baseline of the 11.2 GHz interferometer. The plan is to compare the atmospheric phase fluctuations determined from the radiometers and from the interferometer as a test of the phase correction scheme. The radiometers also allow, under computer control, complete movement of the beam across the sky.

These radiometers are double-side band heterodyne receivers with three detection bands spaced 1.2, 4.5, and 7.5 GHz away from the line centre. The three-channel spectrum measures the water line shape and intensity. The amount of precipitable water vapour is then determined by fitting to an atmospheric model (Wiedner 1998).

The mixers are of the sub-harmonically pumped Shottky types developed at the *Rutherford and Appleton Laboratories*, in the UK. This design has two main advantages: it does not require an external bias and we do not need to double the Gunn oscillator frequency to pump the mixer. The resulting RF circuit is simpler and more reliable. In the laboratory, the receiver temperature was

measured to be about 1500 K. This has been confirmed during normal operation in the field.

The local oscillator (LO) is a free-running, 91.7-GHz Gunn oscillator. It is not phase locked because of the broadness of the water line and because the line is very symmetric. Hence any instability is compensated by the DSB detection. Also the frequency stability of the oscillator is better than 4 MHz/°C, so by regulating the LO temperature to within 1 °C, we obtain a negligible 0.004% frequency drift.

The radiometers are continuously calibrated by switching the beam between the sky and two reference black bodies at temperatures of 35 and 100 °C.

#### 4. Results

Daily climatology data have been collected for the period June–September 1998 winter season in the Southern Hemisphere, and are presented as an average over this period. Figure 5 shows the diurnal cycle of the solar radiation for June–September 1998. The radiation peaks at about 1000 W/m<sup>2</sup>, and the average maximum is around 800 W/m<sup>2</sup>. The histograms in Figure 6 show that the wind is a constant in the area, with lower speeds during the night (median of about 6 m/s) and higher speeds during the day (median of about 10 m/s). This is a parameter that must be kept in mind during the design stage of mechanical structures to be built in the area, especially the antennas. Over 80% of the time the wind

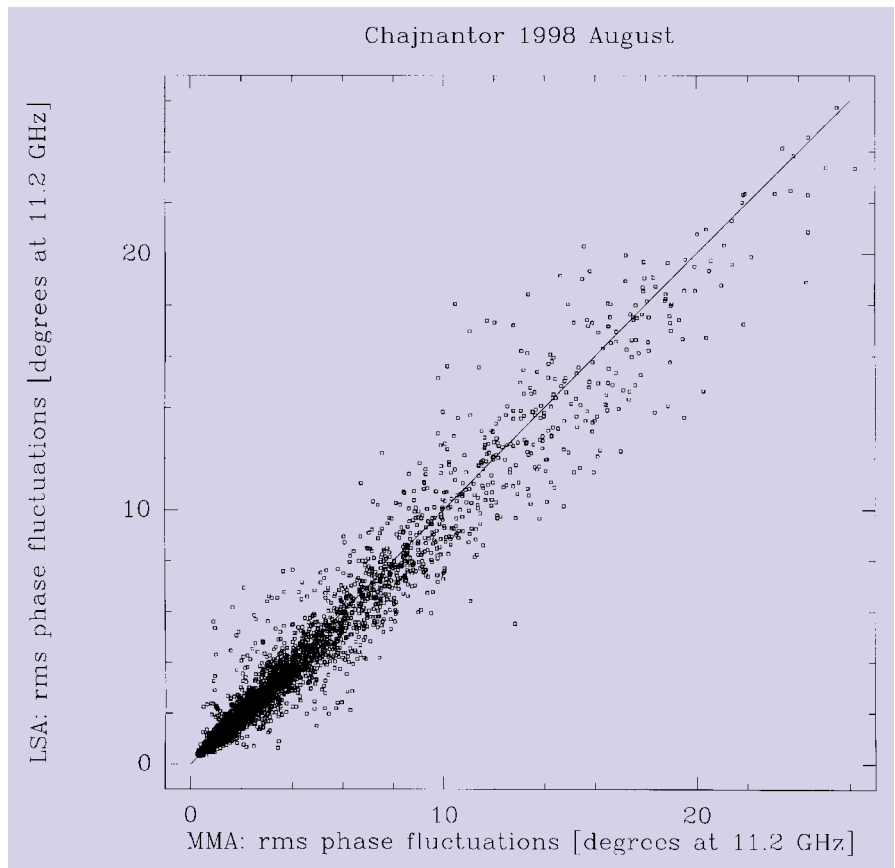


Figure 11: Data from the LSA and the MMA 11.2-GHz interferometers (phase stability monitors) for August 1998. The good correlation between both instruments shows that they perform identically.

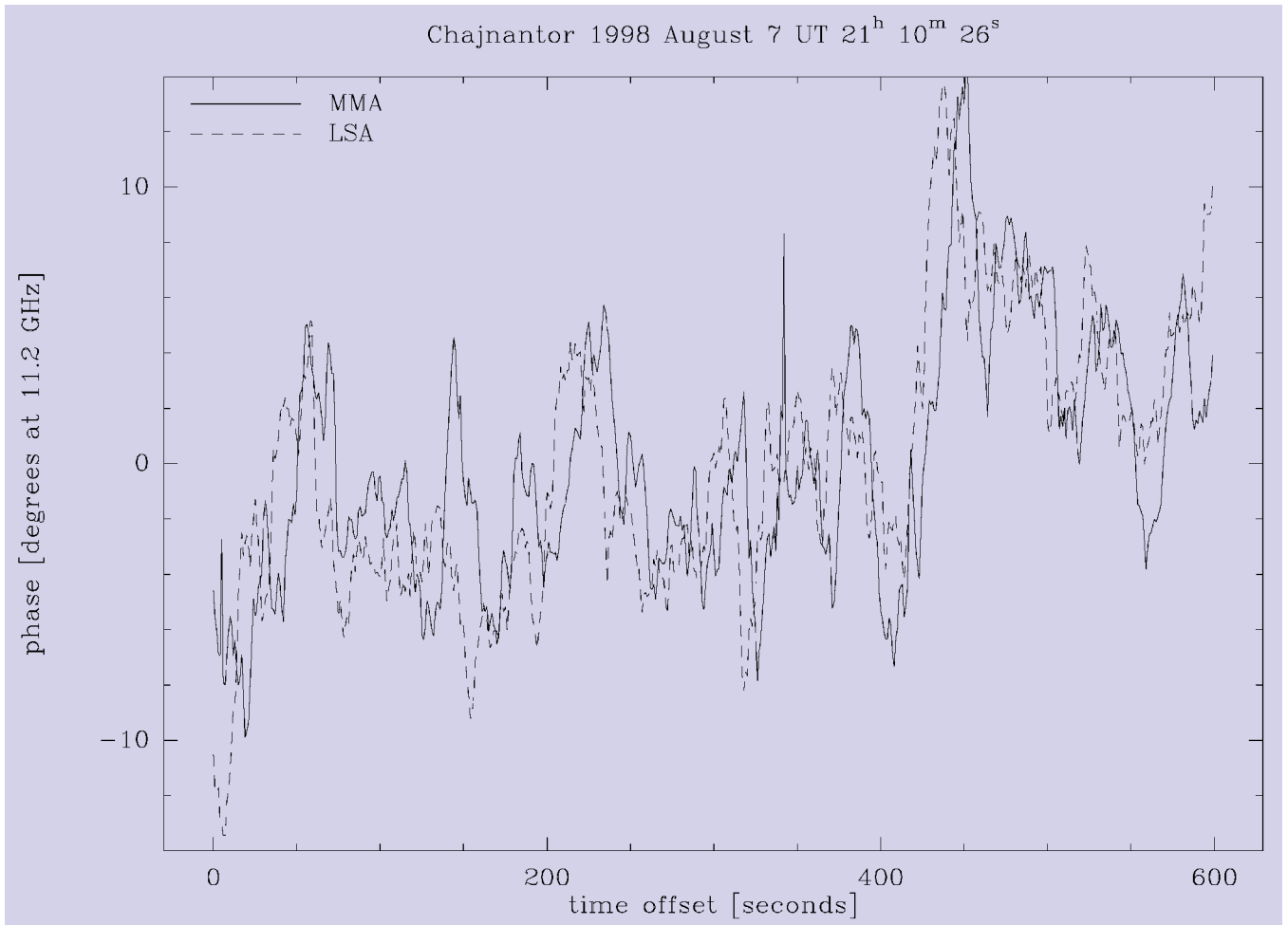


Figure 12: Example of the 11.2-GHz interferometers data showing the expected time delay as the atmospheric turbulence patterns cross over the interferometer line of sight. From these data a height of about 500 m for the turbulence layer can be inferred.

blows from the west (from the desert to the high mountains) as can be seen in Figure 7. The diurnal cycle of temperature is shown in Figure 8: during the night, the temperature becomes stable with the high solar radiation influencing it during the day.

Over the observation period the relative humidity did not change much during a diurnal cycle, being very stable during the night – at an average of around 38% – decreasing during the day to reach a minimum average of around 25%. Figure 9 shows the cumulative function and histogram for the relative humidity.

Data for the precipitable water-vapour (PWV) content of the atmosphere during September 1998 are shown in Figure 10, where some days with very bad weather can be seen as peaks distribution. It can also be seen that normally PWV is lower and stable during local night-time. In the same Figure the histogram for PWV shows that 50% of the time PWV is less than 1 mm and 75% of the time less than 1.7 mm. Since the first analysed month for Chajnantor (September) was a particularly bad month, with several storms over the area, due to a transition between the two global weather conditions known as “El Niño” and “La Niña”, better results are expected after some accumulated

statistics. It should be noted that above 3.5 mm of PWV, measurements are no longer linear due to instrumental limitations.

Data from the two interferometers for August 1998 show they perform identically. The rms phase fluctuations calculated over 10-minute intervals for each interferometer are compared in Fig. 11. Most of the scatter in this figure is due to atmospheric evolution on short time scales. Although the computers controlling the instruments are synchronised to better than 1 s, the 10-minute intervals used for analysis are only synchronised to 5 minutes. The MMA interferometer measures slightly larger fluctuations than the LSA instrument, largely because the MMA interferometer observes a satellite at lower elevation (Holdaway and Ishiguro 1995).

A detailed example of the interferometer data (Fig. 12) shows the expected time delay as the (quasi-static) atmospheric turbulence pattern passes sequentially through the interferometers’ lines of sight. In this example, the LSA signal leads the MMA signal by about 10 s. Together with the geometry and an estimate of the wind speed aloft, we can estimate the height of the dominant turbulent layer. Other

structures are also evident in the data, possibly due to layers at different heights or to fast evolution of the turbulent pattern.

## 5. Conclusions and Future Work

On Llano de Chajnantor we have installed weather stations, two 183 GHz water vapour radiometers, and a phase stability monitor (11.2 GHz interferometer). Data are recorded automatically and retrieved once a month during periodic visits to the site. Data processing and analysis are in their first stages. The meteorological data are analysed in Chile, the 183 GHz radiometer data are analysed in Chile and Sweden, and the interferometer data are analysed in collaboration with NRAO.

The site remains extremely promising for submillimetre interferometry although bad weather caused by the transition between the two global weather conditions known as “El Niño” and “La Niña” was experienced.

In the near future we will compare our data with those obtained through radio sonde launches – a campaign which started in October 1998 and will continue through 1999. This is a collaboration between ESO, NRAO, Cor-

nell University, and the *Smithsonian Astrophysical Observatory*. As a complement to the 183 GHz radiometers, we also plan to install a 22-GHz radiometer to observe another water vapour line and correlate measurements. The radiometer, on loan from R. Martin from *Steward Observatory*, will be installed next year. It has been extensively upgraded to make it more reliable and capable of automatic operation at the site.

In the data analysis, we will explore alternatives to the atmospheric model fitting of the retrieved line from the 183 GHz radiometer measurements, as well as to correlate these measurements with other ones done at different frequencies and/or techniques.

Together with IRAM engineers, we will start measurements of the wind sampled at a high rate in order to determine the power spectrum of the wind behaviour. Such information has an important bear-

ing on the design of the LSA/MMA antennas.

The data, results and all relevant information about the project can now be found in the web page <http://puppis.ls.eso.org/lisa/lisahome.html>

## 6. Acknowledgements

Many people around the world have made fundamental contributions to this project. We wish particularly to thank the ESO staff in Chile, Patricia Adiazola, Viviana Alcayaga, Mary Bauerle, Alfredo Carvajal, Manuel Hervias, Luís Morales, Patricia Parada, and Ivonne Riveros for their special assistance whenever we came with an urgent request.

## References

- Aceituno P., Montecinos A., Departamento de Geofísica Universidad de Chile, 1996.  
*The Messenger*, No. 91, March 1998.  
 Fuenzalida R., ESO internal report, 1996.

- Fuenzalida H., Ruttlant J., in Proceedings of the II Congreso Interamericano de Meteorología, Buenos Aires, Argentina, 1987, 6.3.1.  
 Holdaway M., Ishiguro M., MMA Memo 127, 1995.  
 Holdaway M., Owen F., MMA Memo 136, 1995b.  
 Holdaway M., Radford S., Owen F., Foster S., MMA Memo 139, 1995c.  
 Holdaway M., Radford S., MMA Memo 196, 1998.  
 Otárola A., Delgado G., Bååth L., in Proceedings of the ESO IRAM NFRA Onsala workshop 11–13/12/95, P. Shaver Ed., Springer Verlag, 1996, 358.  
 Radford S., Reiland G., Shillue B., PASP, No. 108, 1996, 441.  
 Schmidt D., PhD thesis, Friedrich-Alexander University, 1997.  
 Wiedner M., PhD thesis, University of Cambridge, 1998.  
 Woody D., Holdaway M., Lay O., Masson C., Owen F., Plambeck D., Radford S., Sutton E., MMA Memo 144, 1995.

gdelgado@eso.org



## **The ISAAC Team on Paranal After First Light on UT1**

From left to right: J. Stegmeier, G. Finger, A. Moorwood, P. Biereichel, J. Brynell, J.-G. Cuby, J. Knudstrup, M. Meyer, J.-L. Lizon.